Proc Indian Natn Sci Acad **79** No. 3 September 2013 pp. 481-492
© *Printed in India.*

Research Paper

Vibrational Spectroscopic, Electronic Structure, Natural Bond Orbital Analysis and Quantum Chemical Investigations of 4-Methoxy-4-Methyl-2-Pentanone

A JAYAPRAKASH*[1], V ARJUNAN[2] and S MOHAN[3]
[1]*Department of Physics, Rajiv Gandhi College of Engineering and Technology, Puducherry 607 402, India*
[2]*Department of Chemistry, Kanchi Mamunivar Centre for Post-Graduate Studies, Puducherry 605 008, India*
[3]*Department of Physics, Hawassa University Main Campus, Hawassa, Ethiopia*

(Received 27 June 2012; Accepted 03 March 2013)

A complete vibrational spectroscopic assignment and analysis of 4-methoxy-4-methyl-2-pentanone has been carried out by using FTIR and FT–Raman spectral data. The fundamental vibrational modes have been proposed on the basis of peak positions, intensities and relative frequencies. The vibrational analysis were also calculated by quantum chemical calculations by hybrid density functional method (B3LYP) with 6-311++G** and cc-pVTZ basis sets. The observed and the calculated frequencies are found to be in good agreement with each other. The most stable geometry of the compound has been determined from the potential energy surface scan. The stable molecular geometry, energy, IR intensities, depolarization ratios and Raman activities are also computed. The electronic exchange interaction and charge delocalisation of the molecule have been determined by natural bond orbital (NBO) analysis. Molecular electrostatic surface potential (MESP), total electron density distribution and frontier molecular orbitals (FMO's) are constructed at B3LYP/6-311++G** level to understand the electronic properties. The electronic properties, such as HOMO and LUMO energies were computed by time–dependent DFT method.

Key Words: 4-Methoxy-4-Methyl-2-Pentanone; FTIR; FT-Raman; DFT; MESP; NBO

1. Introduction

4-Methoxy-4-methyl-2-pentanone (4M4M2PO) with molecular formula ($C_7H_{14}O_2$) is a colourless liquid with high melting point in the range 147-163°C. It is flammable, toxic by ingestion, inhalation or skin absorption. It can be derived from diacetone alcohol. It is used as solvent for a variety of resin coatings, in the manufacture of vinyl resins, insect repellent, paint and varnish-removers and roll-coating inks. Owing to its wide industrial applications a detailed structural and vibrational spectroscopic investigations on 4-methoxy-4-methyl-2-pentanone has been undertaken.

Density functional theory (DFT) is useful and reliable method for studying the physical and chemical properties of molecules. DFT recovers electron correlation in the self-consistent Kohn-Sham procedure through the functions of electron density; hence it is most effective and reliable method. The DFT/B3LYP model exhibits good performance on electron affinities, predicting bond energies and on vibrational frequencies and geometries of organic compounds [1-3].

To the best of our knowledge, structural and vibrational studies using FTIR and FT-Raman spectra,

**Author for Correspondence: E-mail: jp4sree@gmail.com; Tel.: 0413-2346585; Mob: 09943323309*

DFT quantum chemical calculations, molecular electrostatic potential along with total density mapping are not reported in the literature for 4M4M2PO. Thus, considering the industrial importance of this compound, an experimental and theoretical density functional theory (DFT) studies were attempt in the present work to obtain a complete, consistent and precise vibrational assignments, structural parameters, electronic and thermodynamic characteristics of 4M4M2PO. The efficacy of FTIR and FT-Raman spectroscopy in the vibrational analysis of 4-methoxy-4-methyl-2-pentanone has been depicted well in the present investigation. The recorded spectra have been analysed in terms of peak positions and intensities to provide some effective information on its fundamental vibrations. The structure of the compound has been optimised and the harmonic vibrational frequencies were determined by DFT/B3LYP method employing 6-311++G** and cc-pVTZ basis sets. The most stable geometry of the compound has been determined by potential energy surface studies. Furthermore, the other molecular properties of 4M4M2PO namely geometrical parameters, energy, frontier orbital energy gap, molecular electrostatic potential, total electron density and dipole moment are also been determined to describe the thermodynamic and electronic properties completely. The present investigation may be helpful in perception of further studies on 4M4M2PO in different field of research.

2. Experiment Details

Pure (spectroscopic grade) 4-methoxy-4-methyl-2-pentanone [$C_7H_{14}O_2$] was obtained from M/S Aldrich Chemicals, USA and used as such without any further purification to record the FTIR and FT-Raman spectra. The FTIR spectrum of this compound has been recorded as neat liquid using CsI windows in the region 3400-400 cm^{-1} using Bruker IFS 66V spectrometer, with a scanning speed of 30 cm^{-1} min^{-1}, spectral width of 2.0 cm^{-1}. The FT-Raman spectrum was also recorded in the same instrument, with a FRA 106 Raman module equipped with Nd:YAG laser source operating at 1.064 μm line with 200 mW power in the wave number range 3400-100 cm^{-1}. The frequencies of all sharp bands are accurate to 2 cm^{-1}.

3. Computational Details

The optimised molecular structural parameters, vibrational frequency and energies of the optimised structure have been determined by utilising Becke's three parameter hybrid functional (B3) [4,5] combined with gradient corrected correlation functional of Lee-Yang-Parr (LYP) [6] with 6-311++G** and correlation consistent polarised valence triple zeta (cc-pVTZ) [7] basis sets on a Intel Core-i3 processor using Gaussian 03W program [8]. Positive values of all calculated vibrational wavenumbers confirmed the geometry to be located on true local minima on the potential energy surface. The B3LYP/6-311++G** method also been used to calculate the thermodynamical parameters like self-consistent field (SCF) energy (a.u), zero point vibrational energy (ZPVE) (kcal.mol^{-1}), rotational constants (GHz), specific heat (C_v) (cal.mol^{-1}.K^{-1}), entropy (S) (cal.mol^{-1}.K^{-1}), dipole moment, μ (Debye), HOMO and LUMO energies (eV).

GaussView 5.0.8 visualisation program [9] has been used to develop the molecular structure, HOMO and LUMO, total electron density and molecular electrostatic potential surfaces.

4. Results and Discussion

4.1 Potential Energy Surface Scan

In order to illustrate the conformational flexibility of the title molecule, the energy profile as a function of torsion angle (O9=C2-C3-C4) was obtained with B3LYP/6-311++G** method is presented in Fig. 1. During the calculation, all the geometrical parameters were simultaneously relaxed while the dihedral angle O9 = C2-C3-C4 is varied in steps of 30° ranging from 0° to 360°. The energy profile as a function of angle of rotation shows the minimum at 0° and 360°, and maximum at 180°. From the potential energy surface (PES) scan two conformers (A) and (B) have been shortlisted with different energies –425.741787 and –425.731974 Hartrees, respectively and are shown in Fig. 2. Thus, the optimised structure (A) correspond to 0° and 360° in the PES scan curve belongs to the most stable geometry of the title molecule. The relative energies of the PES scan map indicate that the conformer (A) is more stable than conformer B by

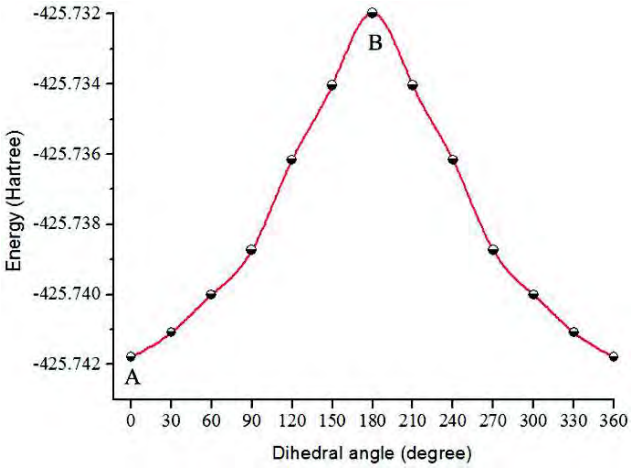

Fig. 1: Molecular energy profile for (O9 = C2-C3-C4) torsion angle of 4-methoxy-4-methyl-2-pentanone

6.158 kcal.mol^{-1}. In the stable conformer (A), the C = O and methylene hydrogen atoms are in the trans position while these are cis in the unstable conformer.

4.2 Optimised Structural Properties

The optimised structure of the molecule obtained by B3LYP/6-311++G** method along with numbering scheme is shown Fig. 3. The B3LYP/6-311++G** method is more consistent and taken for correlation and further discussion. The optimised geometric parameters (bond lengths and bond angles) calculated by 6-311++G** and cc-pVTZ basis sets are listed in Table 1. However, the effects of basis sets are not noticeable for these parameters. The maximum deviation between the bond distances and bond angles computed by the chosen basis sets (6-311++G** and cc-pVTZ) is 0.004Å and 0.24°, respectively and is very minimal. The calculated bond lengths C1-C2 (1.519Å), C-H(methyl) (1.093Å), C-O (1.452Å) and C2 = O9 (1.213Å) are very close to the experimental values 1.507, 1.1, 1.4 and 1.222Å, respectively reported in the literature [2, 3, 10-12].

4.3 Thermodynamic Analysis

In order to understand the thermodynamic behaviour of the title compound, the thermodynamic parameters (such as zero point vibrational energy, thermal energy, specific heat capacity, rotational constants, entropy, and dipole moment) of 4M4M2PO are calculated by

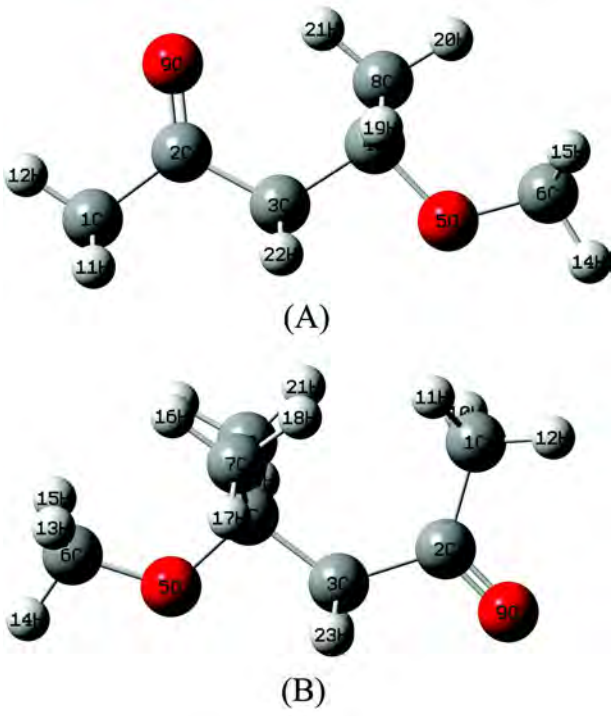

Fig. 2: The possible optimized geometrical conformers (A) and (B) for 4-methoxy-4-methyl-2-pentanone from B3LYP/6-311++G**

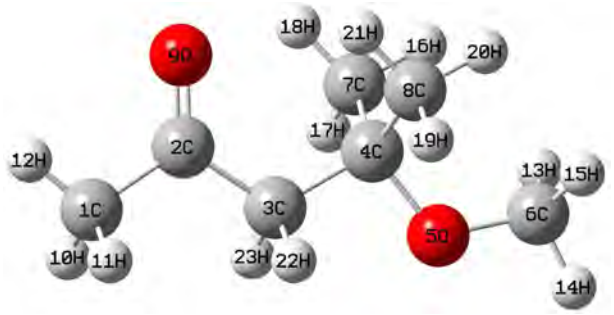

Fig. 3: Optimized molecular structure of 4-methoxy-4-methyl-2-pentanone

DFT/B3LYP method using 6-311++G** and cc-pVTZ basis sets at 298.15 K and 1 atm pressure and presented in Table 2. These functions describe the thermodynamic stability of system at given conditions of pressure and temperature [13]. The total thermal energies, vibrational energy contribution to the total energy and rotational constants values are slightly overestimated in cc-pVTZ basis set than that of 6-311++G** basis set.

Table 1: Optimised geometrical parameters of 4-methoxy-4-methyl-2-pentanone Computed at B3LYP-6-311++G/cc-pVTZ basis sets**

Parameter	B3LYP/ 6-311++G**	B3LYP/ cc–pVTZ	Parameter	B3LYP/ 6-311++G**	B3LYP/ cc–pVTZ
	Bond length (Å)			Bond Angle (degree)	
C1-C2	1.519	1.516	O5-C6-H14	105.9	106.1
C2-C3	1.521	1.518	O5-C6-H15	112.5	112.7
C2-O9	1.213	1.211	H13-C6-H14	108.4	108.3
C3-C4	1.539	1.536	H13-C6-H15	108.9	108.7
C4-O5	1.452	1.448	H14-C6-H15	108.4	108.3
C4-C7	1.534	1.531	H16-C7-H17	108.3	108.3
C4-C8	1.534	1.531	H16-C7-H18	107.8	107.8
O5-C6	1.417	1.413	H17-C7-H18	108.9	109.0
C1-H[a]	1.093	1.090	H19-C8-H20	108.3	108.3
C6-H[b]	1.094	1.092	H19-C8-H21	108.9	109.0
C7-H[c]	1.092	1.090	H20-C8-H21	107.8	107.8
C8-H[d]	1.092	1.090	C2-C1-H[a]	110.2	110.2
C3-H(22,23)	1.097	1.094	C4-C7-H[c]	110.6	110.6
Bond Angle (degree)			C4-C8-H[d]	110.6	110.6
H10-C1-H11	106.9	106.8	C2-C3-H(22,23)	107.7	107.7
H10-C1-H12	109.7	109.7	C4-C3-H(22,23)	108.3	108.3
H11-C1-H12	109.7	109.7	Dihedral angle(degree)		
C1-C2-C3	115.1	115.1	H12-C1-C2-C3	–179.7	–179.8
C1-C2-O9	121.0	120.9	H12-C1-C2-O9	0.29	0.239
C3-C2-O9	123.9	124.0	C1-C2-C3-C4	–179.8	–179.8
C2-C3-C4	119.2	119.3	C1-C2-C3-H22	–56.02	–55.98
H22-C3-H23	104.7	104.6	C1-C2-C3-H23	56.37	56.28
C3-C4-O5	100.9	101.0	O9-C2-C3-C4	0.16	0.137
C3-C4-C7	111.3	111.3	C2-C3-C4-O5	179.9	179.9
C3-C4-C8	111.3	111.3	C2-C3-C4-C7	–62.58	–62.50
O5-C4-C7	110.7	110.7	C2-C3-C4-C8	62.48	62.42
O5-C4-C8	110.7	110.7	H22-C3-C4-O5	56.43	56.39
C7-C4-C8	111.5	111.4	C3-C4-O5-C6	179.9	179.9
C4-O5-C6	118.2	118.2	C7-C4-O5-C6	62.03	62.01
O5-C6-H13	112.5	112.7	C8-C4-O5-C6	–62.13	–62.12

H[a] – H(10,11,12); H[b] - H(13,14,15); H[c] - H(16,17,18); H[d] - H(19,20,21)

Table 2: Calculated thermodynamic parameters of 4-methoxy-4-methyl-2-pentanone at 298.15 K

Thermodynamic parameters		B3LYP/ 6-311++G(d,p)	B3LYP/ cc-pVTZ
SCF energy (a.u)		–425.74193	–425.77578
Total Energy (thermal), E_{total} (kcal.mol^{-1})		132.290	132.387
Vibrational energy, E_{vib} (kcal.mol^{-1})		130.513	130.61
Zero point vibrational energy (kcal.mol^{-1})		125.50862	125.61321
Rotational constants (GHz)	X	3.143	3.157
	Y	0.9069	0.9104
	Z	0.8435	0.8466
Specific heat, C_v (cal.mol^{-1}.K^{-1})		39.404	39.366
Entropy, S (cal.mol^{-1}.K^{-1})		100.56	100.39
Dipole moment, μ (Debye)	μ_x	0.4740	0.4082
	μ_y	–1.4591	–1.4997
	μ_z	0.3880	0.0006
	μ_{total}	1.5824	1.5542

The dipole moment of a molecule is an important property and it helps to study the intermolecular interactions involving the non bonded type dipole-dipole interactions, because higher the dipole moment, stronger the intermolecular interactions [14]. Furthermore, dipole moment can be used to describe the charge movement across the molecule. Direction of the dipole moment vector in a molecule depends on the centers of negative and positive charges. The dipole moment of 4M4M2PO obtained in 6-311++G** basis set is 1.5824 D whereas it is equal to 1.5542 D in cc-pVTZ basis set.

4.4 Electronic Properties

The frontier molecular orbitals, HOMO and LUMO, and frontier orbital energy gap helps to exemplify the reactivity and kinetic stability of the molecules, and are important parameters for electronic studies [15, 16]. The HOMO is the orbital that primarily acts as an electron donor and the LUMO is the orbital that largely acts as the electron acceptor. The energetic behaviour of the title compound has been evaluated by using B3LYP/6-311++G** method and the energies of HOMO, LUMO and their orbital energy gap are found to be –0.2598, –0.0308 and 0.229 eV, respectively. The pictorial illustration of frontier molecular orbitals is shown in Fig. 4.

The positive phase is represented in red and the negative phase is green colour. It can be seen from the MO plots that both $\pi \rightarrow \pi^*$ and $n \rightarrow \pi$ electronic transitions are most probable. The low energy gap of E_{LUMO}–E_{HOMO} confirm the above said eventual charge transfer interaction. Molecular electrostatic potential mapping (MESP) is very useful in the investigation of the molecular structure with its physiochemical property relationships [17].

The MESP is a stratagem of electrostatic potential mapping onto the iso-electron density surface simultaneously displays molecular shape, size and electrostatic potential values and it has been plotted for molecule under investigation using B3LYP/6-311++G** method.

The colour scheme for the MESP surface is red, electron rich, partially negative charge; blue, electron deficient, partially positive charge; light blue, slightly electron deficient region; yellow, slightly electron rich region, respectively.The MESP surface of 4M4M2PO reveals that the region around the

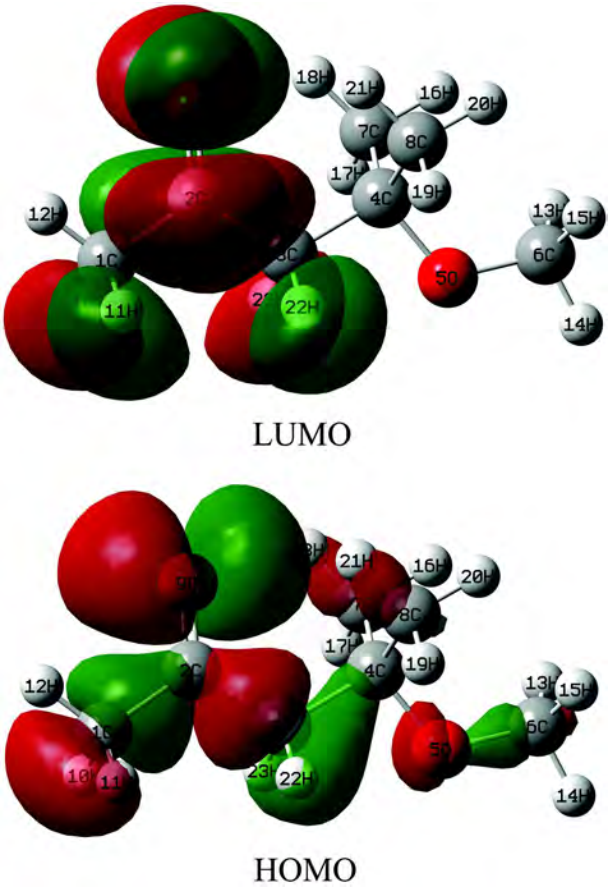

Fig. 4: 3D plot of Frontier molecular orbitals of 4-methoxy-4-methyl-2-pentanone at B3LYP/6-311++G level**

carbonyl oxygen atom represents the most negative potential (red). The hydrogen atoms attached to the ends of the molecular chain beat the maximum bang of positive charge (blue). The MESP surface of 4M4M2PO clearly shows the neuclophilic attack at the carbonyl carbon atom characterised by blue colour. The predominance of green region in the MESP surfaces corresponds to a potential halfway between the two extremes red and dark blue colour. The total electron density, electrostatic potential surfaces (most negative potential –0.04702 eV and most positive potential 0.02657 eV) determined from B3LYP/6-311++G** method are shown in Fig. 5.

4.5 NBO: Perturbation Theory Energy Analysis

The Natural bond orbital (NBO) method demonstrates the bonding concepts like atomic charge, Lewis structure, bond type, hybridisation, bond order, charge

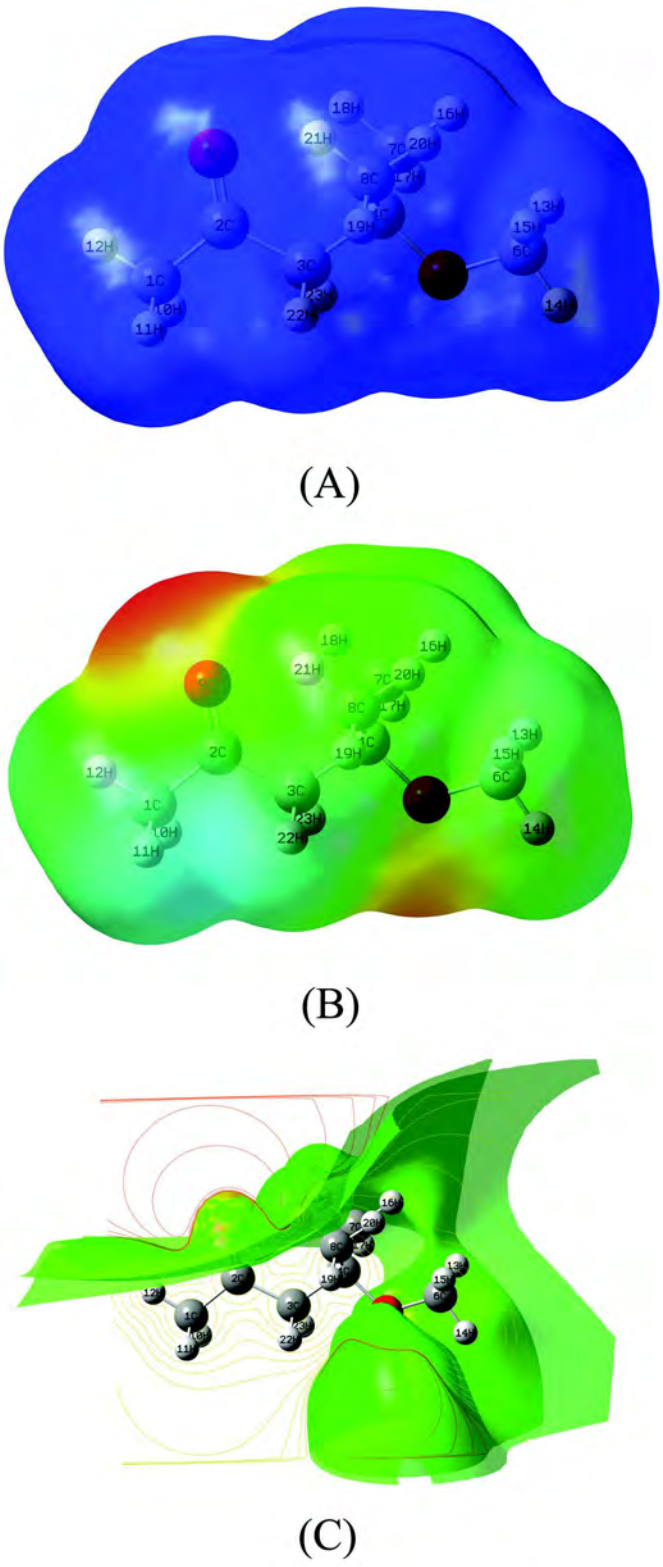

Fig. 5: 3D plot of (A) Total density iso surface, (B) Total density mapped with electrostatic potential surface and (C) ESP contour map of 4-methoxy-4-methyl-2-pentanone

transfer and resonance. NBO analysis is a useful tool for understanding delocalisation of electron density from occupied Lewis-type (donor) NBOs to unoccupied non-Lewis type (acceptor) NBOs within the molecule.

The stabilisation of orbital interaction is proportional to the energy difference between interacting orbitals. Therefore, the interaction having strongest stabilisation takes place between effective donors and effective acceptors. This bonding-anti bonding interactions can be quantitatively described in terms of the NBO approach that is expressed by means of second-order perturbation interaction energy $E^{(2)}$ [18-20]. The stabilisation energy $E^{(2)}$ associated with i (donor) –j (acceptor) delocalisation is estimated from the second-order perturbation approach as [21] given below :

$$E^{(2)} = q_i \frac{F^2(i,j)}{\varepsilon_j - \varepsilon_i}$$

where, q_i is the donor orbital occupancy, ε_i and ε_j are diagonal elements (orbital energies) and F(i,j) is the off–diagonal Fock matrix element. Table 3 lists the calculated second order interaction energies ($E^{(2)}$) above 2.0 kJ.mol^{-1} between the donor–acceptor orbital's of 4M4M2PO. In 4M4M2PO molecule, the bond pair donor orbital, $\sigma_{CH} \rightarrow \pi^*_{CO}$ interaction between the C3–H23 bond pair and the antiperiplanar C2–O9 anti bonding orbital give more stabilisation of 5.25 kJ. mol^{-1}.

The lone pair donor orbital, $n_O \rightarrow \sigma^*_{CC}$ interaction between the oxygen (O9) lone pair and the antiperiplanar C1-C2 anti bonding orbital gives a very strong stabilisation of 20.46 kJ. mol^{-1} while the $n_O \rightarrow \sigma^*$ stabilisation energy of lone pair of electrons present in the oxygen atom (O9) to the anti bonding orbital (σ^*) of C2-C3 is 20.02 kJ.mol^{-1}. These interactions clearly indicate the more stabilisation energy favours electron delocalisation.

4.6 Vibrational Spectral Analysis

The 4M4M2PO molecule posses C_s point group symmetry having two symmetry species namely A' (in-plane) and A" (out of plane). The distribution of 63 normal modes into the irreducible representation for the C_s symmetry is given by $\Gamma_{Vib.} = 39A' + 24A''$. All the vibrations are active in both IR and Raman. Vibrational assignments have been performed with FTIR and FT–Raman spectra and on the theoretically predicted scaled wavenumbers by B3LYP method using 6-311++G** and cc-pVTZ basis sets and are presented in Table 4. The experimental FTIR and FT-Raman spectra are shown in Fig. 6.

As DFT hybrid B3LYP functional tends to overestimate the fundamental vibrational modes, the computed frequencies are scaled by a single scale factor 0.948 in order to bring harmonising with the observed wavenumbers [22]. Calculated vibrational spectral IR intensities and Raman activities of the title molecule for corresponding modes by B3LYP methods with 6-311++G** and cc-pVTZ basis sets are given in Table 4. The scale factor used minimise the root-mean square difference between the calculated and experimental frequencies for the vibrational modes significantly.

4.6.1. Stretching Vibrations

The carbonyl C = O stretching vibration in the ketone molecules is reported near 1700 cm^{-1} in the literature. Accordingly, C = O stretching mode is assigned to

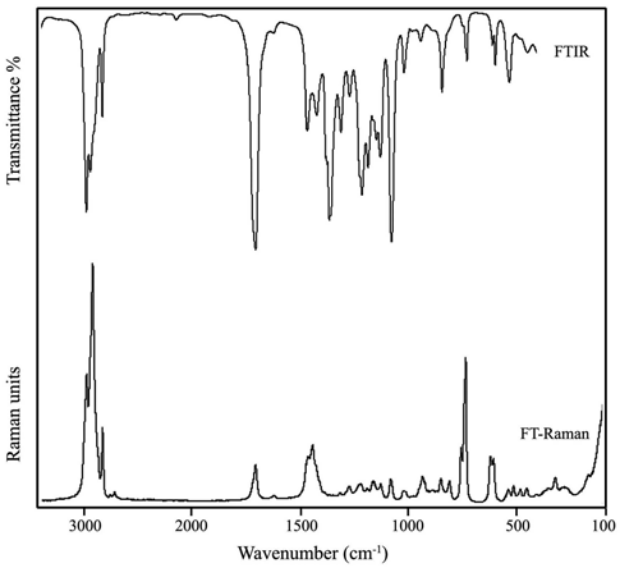

Fig. 6: Experimental FTIR and FT-Raman spectra of 4-methoxy-4-methyl-2-pentanone

Table 3: Second order perturbation theory analysis of 4-methoxy-4-methyl-2-pentanone by Fock matrix in NBO analysis

Donor (i) →Acceptor (j)	$E^{(2)a}$ (kJ mol^{-1})	E(j)-E(i)[b] (a.u.)	F(i, j)[e] (a.u.)
s(C1–H10) →s*(C2–O9)	2.12	1.13	0.044
s(C1–H10) →p*(C2–O9)	4.75	0.53	0.046
s(C1–H11) →s*(C2–O9)	2.08	1.13	0.043
s(C1–H11) →p*(C2–O9)	4.82	0.53	0.046
s(C1–12) →s*(C2–C3)	3.69	0.9	0.052
s (C3–C4) →s*(C5–C6)	3.13	0.92	0.048
s (C3–H22) →s*(C2–O9)	2.5	1.11	0.047
s(C3–H22) →p*(C2–O9)	5.2	0.51	0.047
s(C3–H22) →s*(C4–C7)	3.76	0.88	0.051
s(C3–H23) →s*(C2–O9)	2.48	1.11	0.047
s(C3–H23) →p*(C2–O9)	5.25	0.51	0.047
s(C3–H23) →s*(C4–C8)	3.76	0.88	0.051
s(C6–H14) →s*(C4–O5)	3.81	0.79	0.049
s(C7–H16) →s*(C3–C4)	3.5	0.87	0.05
s(C7–H17) →s*(C4–C8)	3.76	0.87	0.051
s(C7–H18) →s*(C4–O5)	5.23	0.77	0.057
s (C8–H19) →s*(C4–C7)	3.76	0.87	0.051
s (C8–H20) →s*(C3–C4)	3.5	0.87	0.05
s (C8–H21) →s*(C4–O5)	5.23	0.77	0.057
n LP (2) (O5) →s*(C6–H14)	2.77	0.95	0.046
n LP (2) (O5) →s*(C4–C7)	5.26	0.67	0.053
n LP (2) (O5) →s*(C4–C8)	5.27	0.67	0.053
n LP (2) (O5) →s*(C6–H13)	6.48	0.68	0.06
n LP (2) (O5) →s*(C6–H15)	6.48	0.68	0.06
n LP (2) (O9) →s*(C1–C2)	20.46	0.65	0.104
n LP (2) (O9) →s*(C2–C3)	20.02	0.66	0.104

[a]Stabilisation (delocalisation) energy.
[b]Energy difference between i(donor) and j(acceptor) NBO orbitals.
[e]Fock matrix element i and j NBO orbitals.

the very strong band observed at 1710 cm^{-1} in FTIR spectrum and calculated at 1709 cm^{-1} [2, 23-25]. Under C_s symmetry the C-C stretching modes assignments are given to the IR and Raman bands found near 1260, 1180, 1150 and 1090 cm^{-1} and are found to be in close agreement with the corresponding calculated values in the range 1250-1098 cm^{-1}. The fundamental modes observed at 1220 and 1030 cm^{-1} in the FTIR along with their closer Raman counterparts are assigned to the C–O and O–CH_3 stretching modes, respectively [3].

4.6.2. Methyl and Methylene Mode Vibrations

Twelve methyl stretching $\nu(CH_3)$ modes were calculated to occur in the range 2976-2841 cm^{-1} (except the wavenumbers 2889 and 2864 cm^{-1} corresponds to methylene modes) at B3LYP level. Very strong to medium intense IR bands observed at 2970, 2940 and 2930 cm^{-1} and their Raman counterparts are of very strong to medium intense bands at 2980 and 2930 cm^{-1} are assigned to methyl stretching modes. The CH_3 asymmetric and symmetric deformations were calculated in the region 1460-1350 cm^{-1} from B3LYP method.

These are all well agree with the observed wavenumbers obtained at 1470, 1435, 1370, 1350 cm^{-1} and 1440, 1375 cm^{-1}, respectively. The calculated value near 1390 cm^{-1} is assigned with CH_2 deformation. In accordance with the literature, rocking and wagging vibrations of CH_3 groups observed near 940 and 845, 800 cm^{-1}, respectively. The twisting and torsion vibrations of CH_3 groups are assigned to the lower wavenumbers calculated below 280 cm^{-1}. Assignments attributed to methyl and methylene group vibrations are in line with the reported data [26, 27].

4.6.3. In-plane and Out-of-Plane Bending Vibrations

Bands of weak intensities observed at 760, 725 and 510 cm^{-1} in Raman spectrum are assigned to C–CH_3 in-plane bending modes, whereas the bands appear at 610 and 325 cm^{-1} are attributed to C=O and O–Me_2 in-plane bending modes, respectively. The out of plane bending modes of C–C and C–O are attributed to the observed bands at 470 and 450 cm^{-1} in Raman spectrum. The in-plane bending vibrations of C–C

Table 4: Observed and calculated wavenumbers for vibrational modes of 4-methoxy-4-methyl-2-pentanone

Spp.	FTIR (cm^{-1})	FT-Raman (cm^{-1})	B3LYP/ 6–311++G**		IR intensity	Raman activity	Depolari-sation	B3LYP/ cc-pVTZ		IR intensity	Raman activity	Assignment
			Unscaled (cm^{-1})	Scaled (cm^{-1})				Unscaled (cm^{-1})	Scaled (cm^{-1})			
(1)	(2)	(3)	(4)	(5)	(6)	(7)	(8)	(9)	(10)	(11)	(12)	(13)
A”			3139	2976	10.44	78.29	0.62	3140	2976	10.30	80.31	ν_aMe_1
A”			3127	2965	10.46	73.19	0.64	3130	2967	10.05	71.15	ν_aMe_3
A”			3123	2961	1.300	14.35	0.75	3126	2963	1.013	13.44	ν_aMe_4
A”	2970vs	2980s	3106	2944	33.21	98.23	0.54	3102	2940	48.35	88.03	ν_aMe_2
A’	2940s	2930vs	3098	2937	47.78	95.80	0.59	3098	2937	31.59	107.9	ν_aMe_3
A’			3096	2935	7.960	35.63	0.75	3096	2935	7.811	34.01	ν_aMe_4
A’			3087	2927	9.860	60.35	0.75	3087	2927	9.650	61.40	ν_aMe_1
A’			3050	2891	51.58	16.36	0.75	3048	2889	39.33	20.99	ν_aMe_2
A”			3048	2889	28.58	58.86	0.75	3045	2886	48.00	50.80	ν_aCH_2
A’		2860m	3039	2881	9.248	413.5	0.01	3041	2883	9.072	357.4	ν_sMe_3
A’			3032	2875	14.01	144.8	0.01	3034	2877	11.41	146.5	ν_sMe_1
A’			3032	2874	11.65	5.048	0.75	3034	2876	4.142	9.600	ν_sMe_4
A’			3021	2864	10.77	6.580	0.55	3022	2864	11.87	9.885	ν_sCH_2
A’	2830m		2997	2841	54.24	101.2	0.02	2997	2841	53.27	97.44	ν_sMe_2
A’	1710vs	1710w	1776	1709	154.4	7.847	0.56	1781	1688	138.3	5.385	νC=O
A”	1470m	1460w	1519	1462	11.31	3.638	0.71	1520	1441	8.849	3.248	δ_aMe_3
A”	1435m	1440m	1515	1458	18.42	5.754	0.72	1517	1438	18.30	6.92	δ_aMe_3
A”			1509	1452	1.834	4.411	0.75	1510	1431	1.641	4.009	δ_aMe_4
A”			1503	1446	1.124	4.326	0.75	1505	1427	1.026	4.336	δ_aMe_2
A’			1487	1431	2.886	1.377	0.75	1489	1411	2.014	1.111	δ_aMe_2
A’			1483	1427	0.2786	16.32	0.75	1484	1407	0.146	17.61	δ_aMe_4
A’			1477	1421	14.05	5.651	0.75	1479	1402	11.21	6.581	δ_aMe_1
A’			1469	1413	4.335	1.063	0.28	1474	1397	0.667	3.399	δ_aMe_1
A’			1467	1411	16.25	12.87	0.73	1468	1391	17.20	11.72	δ_sMe_2
A’			1445	1390	3.089	5.084	0.75	1446	1371	2.610	5.178	δ_sCH_2
A’	1370s		1410	1356	30.76	0.1487	0.07	1411	1338	28.70	0.2457	δ_sMe_3
A’			1394	1341	23.03	0.2257	0.75	1396	1323	20.64	0.2321	δ_sMe_4
A’	1350s		1388	1335	64.87	0.2673	0.64	1390	1317	57.48	0.6177	δ_sMe_1
A’	1310m		1367	1315	56.76	2.506	0.66	1367	1296	56.71	2.865	νC–C
A’	1260w	1260w	1298	1248	8.625	4.377	0.75	1298	1230	8.040	3.410	νC–C

Table 4 contd ...

Continuation of Table 4

(1)	(2)	(3)	(4)	(5)	(6)	(7)	(8)	(9)	(10)	(11)	(12)	(13)
A’	1220m	1225vw	1284	1235	11.75	5.771	0.73	1285	1218	12.34	4.892	νC–O
A’	1180m	1175vw	1203	1157	21.77	1.158	0.53	1207	1144	22.62	0.6542	νC–C
A’	1150m	1140vw	1197	1152	12.67	2.232	0.53	1201	1138	10.44	2.515	νC–C
A’			1169	1125	5.167	0.964	0.75	1176	1115	4.063	1.180	ρCH_2
A’			1163	1119	5.234	6.767	0.75	1165	1105	7.165	4.682	ρMe_2
A’	1090vs	1080vw	1155	1111	124.9	2.003	0.65	1158	1098	124.0	1.546	νC–C
A’	1030vw		1093	1051	112.2	8.672	0.30	1098	1041	110.9	8.281	νC–O
A’			1043	1003	0.3941	3.156	0.75	1046	992	0.430	2.980	ρMe_4
A’			1019	981	1.104	4.181	0.56	1020	967	1.443	4.035	ρMe_3
A’	950vw	940vw	993	955	1.393	0.059	0.75	995	943	1.280	0.0614	ρMe_1
A”			935	900	24.50	3.659	0.21	936	887	26.29	3.370	ωMe_3
A”			926	891	0.013	2.797	0.75	927	879	0.001	2.462	ωMe_4
A”	845w	850vw	882	849	10.48	9.041	0.45	883	837	11.20	8.546	ωMe_2
A”		800vw	820	789	0.3838	0.4437	0.75	822	780	0.464	0.3514	ωMe_1
A’	740vw	760w	812	781	10.46	3.439	0.35	815	772	8.903	3.410	β$C–Me_1$
A’		725m	750	721	2.175	8.515	0.10	751	712	1.350	8.049	β$C–Me_3$
A’	610 vw	610vw	615	591	13.96	7.740	0.17	615	583	14.35	7.441	βC=O
A’	520 vw	510vw	528	508	10.26	1.419	0.34	529	501	10.49	1.123	β$C–Me_4$
A”		470vw	487	469	0.2030	0.9759	0.75	489	463	0.239	1.038	γC–C
A”	440 vw	450vw	439	423	4.878	0.3020	0.75	439	416	4.186	0.2673	γO–C
A’			394	379	1.312	0.3591	0.22	393	373	1.076	0.2427	βC–C
A’		325vvw	358	344	0.2346	3.264	0.16	358	339	0.313	3.010	β$O–Me_2$
A”			333	320	0.895	0.1951	0.75	332	315	0.788	0.1157	γC–C
A’			309	298	0.631	1.979	0.21	309	293	0.563	1.760	βC–C
A’			285	275	1.098	0.4987	0.69	284	269	1.221	0.6242	βC–O
A”			272	261	4.216	0.1344	0.75	267	253	4.230	0.1076	τMe_3 twisting
A”			253	244	0.2953	0.0736	0.72	251	238	0.219	0.0463	τMe_4 twisting
A”			181	174	2.252	0.0792	0.75	178	169	1.808	0.0947	τMe_1 twisting
A”			152	146	7.107	0.5076	0.63	152	144	6.418	0.5168	γ$C–CH_3$
A”			106	102	4.883	0.4946	0.75	108	102	4.383	0.3392	γ$C–CH_3$
A”			85	81	0.390	0.1209	0.75	94	89	0.001	0.1504	τMe_2 twisting
A”			51	49	2.929	0.3312	0.75	51	48	2.441	0.3791	τMe_1 torsion
A”			38	36	1.201	0.7924	0.75	25	23	1.301	0.77	τMe_2 torsion

Me_1– C1,H(10,11,12); Me_2– C6,H(13,14,15); Me_3– C7,H(16,17,18); Me_4– C8,H(19,20,21);
vs–very strong, s–strong, m–medium, w–weak, vw–very weak;
ν–stretching, α–deformation, β–in plane bending, γ–out of plane bending, ρ–rocking, ω-wagging and τ–twisting/torsion

and C–O are assigned in the lower frequency region 390-285 cm^{-1} [2, 26-29].

All the observed vibrational frequency of the fundamental modes of the title compound are in close agreement with the scaled calculated values determined by B3LYP method using 6-311++G** and cc-pVTZ basis sets.

5. Conclusion

In the present work, the potential energy surface scan calculation as a function of torsion angle (O9 = C2-C3-C4) was carried and the most stable geometry of the compound (structure A) is confirmed. A detailed vibrational analysis with experimental and theoretical spectral data, thermodynamic properties, molecular electrostatic potential surface scan calculations, total electron density distribution and frontier molecular orbital HOMO and LUMO analysis of industrially important 4M4M2PO molecule were carried out at B3LYP level with 6-311++G** and cc-pVTZ basis sets. The calculated HOMO, LUMO and their energy gap values along with their plot have presented for better understanding of charge transfer interactions within the molecule. The various parameters computed among DFT methods are compared and considerable level of correlation is noticed between the opted methods. Comparison between the experimental and theoretical results indicates that density functional B3LYP method is able to provide satisfactory results for predicting vibrational wavenumbers and the structural parameters of 4M4M2PO molecule. The results prove the ability of the methodology (DFT) for elucidation vibrational spectra of the title molecule and exceptional understanding of thermodynamic and electronic properties.

References

1. Jayaprakash A, Arjunan V and Mohan S *Spectrochim Acta A* **81** (2011) 620
2. Jayaprakash A, Arjunan V, Sujin P Jose and Mohan S *Spectrochim Acta A* **83** (2011) 411
3. Arjunan V, Suja Ravi Issac A, Rani T, Mythili CV and Mohan S *Spectrochim Acta A* **78** (2011) 1625
4. Becke AD *Phys Rev A* **38 (**1988) 3098
5. Becke AD *J Chem Phys* **98** (1993) 5648
6. Lee C, Yang W and Parr RG *Phys Rev B* **37** (1988) 785
7. Dunning TH Jr *J Chem Phys* **90** (1989) 1007
8. Frisch MJ, Trucks GW, Schlegel HB, Scuseria GE, Robb MA, Cheeseman JR, Montgomery JA Jr, Vreven T, Kudin KN, Burant JC, Millam JM, Iyengar SS, Tomasi J, Barone V, Mennucci B, Cossi M, Scalmani G, Rega N, Petersson GA, Nakatsuji H, Hada M, Ehara M, Toyota K, Fukuda R, Hasegawa J, Ishida M, Nakajima T, Honda Y, Kitao O, Nakai H, Klene M, Li X, Knox JE, ratchian HP, Cross JB, Adamo C, Jaramillo J, Gomperts R, Stratmann RE, Yazyev O, Austin AJ, Cammi R, Pomelli C, Ochterski JW, Ayala PY, Morokuma K, Voth GA, Salvador P, Dannenberg JJ, Zakrzewski VG, Dapprich S, Daniels AD, Strain MC, Farkas O, Malick DK, Rabuck AD, Raghavachari K, Foresman JB, Ortiz JV, Cui Q, Baboul AG, Clifford S, Cioslowski J, Stefanov BB, Liu G, Liashenko A, Piskorz P, Komaromi I, Martin RL, Fox DJ, Keith T, Al-Laham MA, Peng CY, Nanayakkara A, Challacombe M, Gill PMW, Johnson B, Chen W, Wong MW, Gonzalez C and Pople JA Gaussian, Inc, Wallingford CT, 2004
9. Frisch AE, Hratchian HP and Dennington RD II *et al*. GaussView Version 5.0.8 Gaussian, Inc. Wallingford CT 2009
10. Xu S, Zhao B, Wang Z and Fan Y *J Mol Struct (Theochem)* **428** (1998) 123
11. Shucheng Xu, Chengdong Wang, Guohe Sha, Jinchun Xie and Zhongzhi Yang *J Mol Struct (Theochem)* **459** (1999) 163
12. Shucheng Xu, Chengdong Wang, Guohe Sha, Jinchun Xie and Zhongzhi Yang *J Mol Struct* (Theochem) **467** (1999) 85
13. Ran Z, Baotong D, Gang S and Yuxi S *Spectrochim Acta Part A* **75** (2010) 1115
14. Prasad O, Sinha L and Kumar N *J At Mol Sci* **1** (2010) 201
15. Fleming I *Frontier Orbitals and Organic Chemical Reactions* John Wiley and Sons New York (1976) pp 5
16. Murray JS and Sen K *Molecular Electrostatic Potentials, Concepts and Applications* Elsevier Amsterdam (1996)
17. Seminario JM *Recent Developments and Applications of Modern Density Functional Theory* Vol 4 Elsevier (1996) pp 800

18. Reed AE and Weinhold F *J Chem Phys* **78** (1983) 4066
19. Reed AE, Weinstock RB and Weinhold F *J Chem Phys* **83** (1985) 735
20. Reed AE and Weinhold F *J Chem Phys* **83** (1985) 1736
21. Foster JP and Weinhold F *J Am Chem Soc* **102** (1980) 7211
22. Andrade SG, Luisa, Goncalves CS and Jorge FE *J Mol Struct (THEOCHEM)* **846** (2008) 20
23. Wilson Jr EB, Decius JC and Cross PC PC *Molecular Vibrations* McGraw Hill New York (1955)
24. Singh DN, Singh ID and Yadav RA *Indian J Phys **76B 3*** (2002) 307
25. Arjunan V, Puviarasan N and Mohan S *Spectrochim Acta A* **64** (2006) 233
26. Silverstein RM, Bassler GC and Morrill TC *Spectrometric Identification of Organic Compounds* 5th Edn (1991) p 245
27. Kuptsov AH and ZhiZhin GN *Handbook of Fourier Transform Raman and Infrared Spectra of Polymers* Elsevier Amsterdam (1998)
28. Shucheng Xu, Chengdong Wang, Guohe Sha, Jinchun Xie and Zhongzhi Yang *J Mol Struct (Theochem)* **467** (1999) 85
29. Zhengyu Zhou, Dongmei Du, Aiping Fu and Qingsen Yu *J Mol Struct (Theochem)* **530** (2000) 149.